Magnetization Switching and Microwave Oscillations in Nanomagnets Driven by Spin-Polarized Currents

G. Bertotti,[1] C. Serpico,[2] I. D. Mayergoyz,[3] A. Magni,[1] M. d'Aquino,[2] and R. Bonin[4,1]
[1]IEN Galileo Ferraris, Strada delle Cacce 91, 10135 Torino, Italy
[2]Dipartimento di Ingegneria Elettrica, Universitá di Napoli "Federico II", via Claudio 21, 80125 Napoli, Italy
[3]Department of Electrical and Computer Engineering, University of Maryland, College Park, Maryland 20742, USA
[4]Dipartimento di Fisica, Politecnico di Torino, Corso Duca degli Abruzzi 26, 10129 Torino, Italy
(Received 7 October 2004; published 1 April 2005)

A novel theoretical approach to magnetization dynamics driven by spin-polarized currents is presented. Complete stability diagrams are obtained for the case where spin torques and external magnetic fields are simultaneously present. Quantitative predictions are made for the critical currents and fields inducing magnetization switching, for the amplitude and frequency of magnetization self-oscillations, and for the conditions leading to hysteretic transitions between self-oscillations and stationary states.

DOI: 10.1103/PhysRevLett.94.127206 PACS numbers: 75.60.Jk, 85.70.Kh

Considerable interest has been generated in recent years by the discovery that a current of spin-polarized electrons can apply appreciable torques to a nanoscale ferromagnet. This mechanism was theoretically predicted in Refs. [1,2]. Subsequently, a number of experiments have shown that spin transfer can indeed induce switching [3–5] or microwave oscillations [6,7] of the magnetization. Significant effort has been devoted to the explanation of these results [8], in view of the new physics involved and of the possible applications to new types of current-controlled memory cells or microwave sources and resonators [6,7]. However, the precise nature of magnetization dynamics when spin-polarized currents and external magnetic fields are simultaneously present has not yet been fully understood.

The spin-transfer-driven nanomagnet is a nonlinear open system that is forced far from equilibrium by the injection of the current. Thus, the appropriate framework for the study of the problem is nonlinear dynamical system theory and bifurcation theory [9]. In this Letter we show that within this framework all the complexity and subtlety of spin-torque effects are fully revealed and quantified once it is recognized that both intrinsic damping and spin transfer can be treated as *perturbations* of the free precessional dynamics typical of ferromagnetic resonance. This leads to detailed analytical predictions which explain many of the features observed in experiments [3–7].

In typical spin-transfer investigations, the electron current is sent along the z direction across a metallic multilayer element with layers parallel to the (x, y) plane. The element consists of a so-called "fixed" magnetic layer with magnetization pinned along the x axis, a nonmagnetic spacer, and a "free" magnetic layer exposed to the torque due to the x-directed spin-polarization that the electrons acquire from the fixed layer. The magnetization dynamics in the free layer is described by the modified Landau-Lifshitz-Gilbert equation proposed in Ref. [1]. This equation can be written in dimensionless form as

$$\frac{d\mathbf{m}}{dt} - \alpha\mathbf{m}\times\frac{d\mathbf{m}}{dt} = -\mathbf{m}\times\left(\mathbf{h}_{\text{eff}} - \beta\frac{\mathbf{m}\times\mathbf{e}_p}{1 + c_p\mathbf{m}\cdot\mathbf{e}_p}\right), \quad (1)$$

where the free-layer magnetization $\mathbf{m}$ and the effective field $\mathbf{h}_{\text{eff}}$ are normalized by the saturation magnetization M_s, time is measured in units of $(\gamma M_s)^{-1}$ (γ is the absolute value of the gyromagnetic ratio), α is the damping constant ($\alpha \lesssim 10^{-2}$ for all materials of interest), the unit vector $\mathbf{e}_p$ gives the direction of the spin polarization (along x in our case), $c_p = (1 + P)^3/[3(1 + P)^3 - 16P^{3/2}]$, and $\beta = 4(J_e/J_p)P^{3/2}/[3(1 + P)^3 - 16P^{3/2}]$. The parameter β is proportional to the current density J_e, taken as positive when the electrons flow from the free into the fixed layer. The parameter P $(0 < P < 1)$ measures the degree of spin polarization [1] whereas $J_p = \mu_0 M_s^2|e|d/\hbar$ (μ_0 is vacuum permeability, e is the electron charge, d is the thickness of the free layer, and $\hbar$ is the Planck constant). For a Co layer 3 nm thick, $J_p \simeq 10^9$ A cm^{-2}, which shows that $\beta \lesssim 10^{-2}$ for the typical current densities employed in experiments. The effective field is given by $\mathbf{h}_{\text{eff}} = -\partial g_L/\partial\mathbf{m}$, where $g_L(\mathbf{m};\mathbf{h}_a)$ is the energy density in the free layer normalized by $\mu_0 M_s^2$:

$$g_L(\mathbf{m};\mathbf{h}_a) = \frac{1}{2}(D_x m_x^2 + D_y m_y^2 + D_z m_z^2) - \mathbf{h}_a\cdot\mathbf{m}. \quad (2)$$

The quadratic term describes shape and crystal anisotropy effects whereas the linear term is due to the interaction with the external field $\mathbf{h}_a$. We assume $D_x < D_y < D_z$, so x is the free-layer easy axis. The energy g_L is not conserved by the magnetization dynamics. Indeed, it can be derived from Eq. (1) that

$$\frac{dg_L}{dt} = -\alpha\left|\frac{d\mathbf{m}}{dt}\right|^2 - \beta\frac{\mathbf{m}\times\mathbf{e}_p}{1 + c_p\mathbf{m}\cdot\mathbf{e}_p}\cdot\frac{d\mathbf{m}}{dt}. \quad (3)$$

When $\mathbf{h}_a$ and β are constant in time, Eq. (1) describes an autonomous dynamical system whose state vector $\mathbf{m}(t)$ evolves on the surface of the unit sphere $|\mathbf{m}|^2 = 1$. The

fact that the state space is two-dimensional has the following general consequences [9]: (i) *chaos is precluded*; (ii) the only possible types of magnetization response are either *stationary modes* associated with static solutions (fixed points) of Eq. (1) or *self-oscillations* associated with periodic solutions (limit cycles) of Eq. (1) (Poincaré-Bendixson theorem [9]).

To understand which of these possibilities may be realized, we notice that due to the smallness of α and β the magnetization dynamics can be viewed as a perturbation of the conservative dynamics corresponding to $\alpha = \beta = 0$. Not only the magnitude of $\mathbf{m}$ but also the energy g_L is conserved when $\alpha = \beta = 0$ [see Eq. (3)]. Accordingly, magnetization trajectories are given by the intersection of the unit sphere with the energy surface $g_L(\mathbf{m}; \mathbf{h}_a) = g_0$ for various g_0. When the field is applied along the easy axis the ensuing phase portrait [10] exhibits mirror symmetry with respect to the (m_x, m_y) plane (Fig. 1). Its projection onto this plane consists of lines, each of which represents two trajectories or two parts of the same trajectory with opposite values of m_z. The separatrices (bold lines) originating from the energy saddle at $m_x = -1$ create a partition of the phase portrait into the two mirror-symmetric high-energy regions H^2 and the low-energy region L around $m_x = 1$. This partition, dependent on $\mathbf{h}_a$ only, is also representative of the actual dynamics for $\alpha \neq 0$ and $\beta \neq 0$, since α and β are too small to alter it in any substantial way.

When no current is injected ($\beta = 0$), the presence of intrinsic damping ($\alpha \neq 0$) forces the energy to decrease for any magnetization motion [see Eq. (3)]. The closed orbits shown in Fig. 1 are transformed into finely spiraling trajectories approaching the energy minimum at $m_x = 1$. This is the only observable magnetization mode under zero current and positive field $h_{ax} > D_y - D_x$; no persistent self-oscillations are possible. The injection of the current

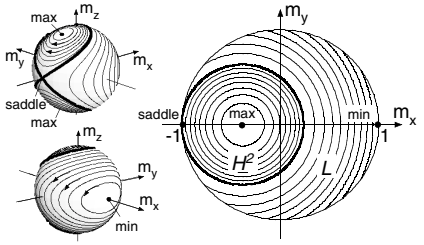

FIG. 1. On the left is a two-sided view of the magnetization unit sphere with a representation of phase portrait for conservative dynamics $d\mathbf{m}/dt = -\mathbf{m} \times \mathbf{h}_{\text{eff}}$ when a field is applied along the x axis and $D_y - D_x < h_{ax} < D_z - D_x$. Vertical projection of phase portrait onto the (m_x, m_y) plane is shown on the right. min: energy minimum at $m_x = 1$; max: symmetric energy maxima.

has quite significant effects. Consider a magnetization motion close to $m_x = 1$. Because of the smallness of α and β, the motion over time intervals of the order of 1 precession period is nearly coincident with one of the constant-energy orbits shown in Fig. 1. Along this orbit $\mathbf{m} \times \mathbf{e}_p$ is approximately opposite to $d\mathbf{m}/dt$, so $dg_L/dt \simeq (K\beta - \alpha)|d\mathbf{m}/dt|^2$, where K is some positive constant. Thus $dg_L/dt > 0$ when $\beta/\alpha \gtrsim 1/K$, which means that at sufficiently large positive currents the state $m_x = 1$ will inevitably become unstable and a limit cycle, that is, persistent self-oscillations will appear [1,2]. Self-oscillations are characterized by the fact that the energy g_L becomes periodic in time; that is, the energy balance over one oscillation period becomes equal to zero. In calculating this balance through Eq. (3) one can use the mentioned fact that in one oscillation period the magnetization trajectory is nearly coincident with a certain orbit of the conservative dynamics. Let us denote this orbit and its energy by $C(g_0)$ and g_0, respectively. The energy balance can be calculated along $C(g_0)$ instead of the actual trajectory without significant error. By also taking into account that $d\mathbf{m}/dt = -\mathbf{m} \times \mathbf{h}_{\text{eff}}$ along $C(g_0)$, one finds that the integral of Eq. (3) over one oscillation period is approximately equal to $-\alpha M(g_0, \mathbf{h}_a, \beta/\alpha)$, where

$$M(g_0, \mathbf{h}_a, \beta/\alpha) = \oint_{C(g_0)} \times \left(-\mathbf{m} \times \mathbf{h}_{\text{eff}} + \frac{\beta}{\alpha} \frac{\mathbf{m} \times \mathbf{e}_p}{1 + c_p \mathbf{m} \cdot \mathbf{e}_p} \right) \cdot d\mathbf{m}. \tag{4}$$

Therefore, it is expected that $M(g_0, \mathbf{h}_a, \beta/\alpha) \simeq 0$ for self-oscillations. These heuristic considerations can be made rigorous by making use of Melnikov theory for slightly dissipative systems [9]. This theory, when applied to Eq. (1), leads to the following fundamental result.

Existence of limit cycles.—In the limit $\alpha \to 0$, $\beta \to 0$, $\beta/\alpha \to$ const, the equation $M(g_0, \mathbf{h}_a, \beta/\alpha) = 0$ represents the *necessary and sufficient* condition for the existence of a periodic solution (limit cycle) of Eq. (1). The limit cycle is asymptotically coincident with a trajectory of energy g_0 of the conservative dynamics $d\mathbf{m}/dt = -\mathbf{m} \times \mathbf{h}_{\text{eff}}$, and is stable (unstable) when $\partial M(g_0, \mathbf{h}_a, \beta/\alpha)/\partial g_0 > 0 (< 0)$.

Based on this result, we have analytically constructed the complete stability diagram for spin-transfer-driven magnetization dynamics. Since $M(g_0, \mathbf{h}_a, \beta/\alpha)$ is a function of β/α, the diagram will not depend on α and β separately, but rather on their ratio β/α. The example shown in Fig. 2 refers to the system investigated in Ref. [7] and reproduces many of the features observed in those experiments. An extremely rich variety of phenomena is predicted depending on whether $h_{ax} < -(D_y - D_x)$, $|h_{ax}| < D_y - D_x$ (this is where current-induced magnetization switching occurs), or $h_{ax} > D_y - D_x$. Here we

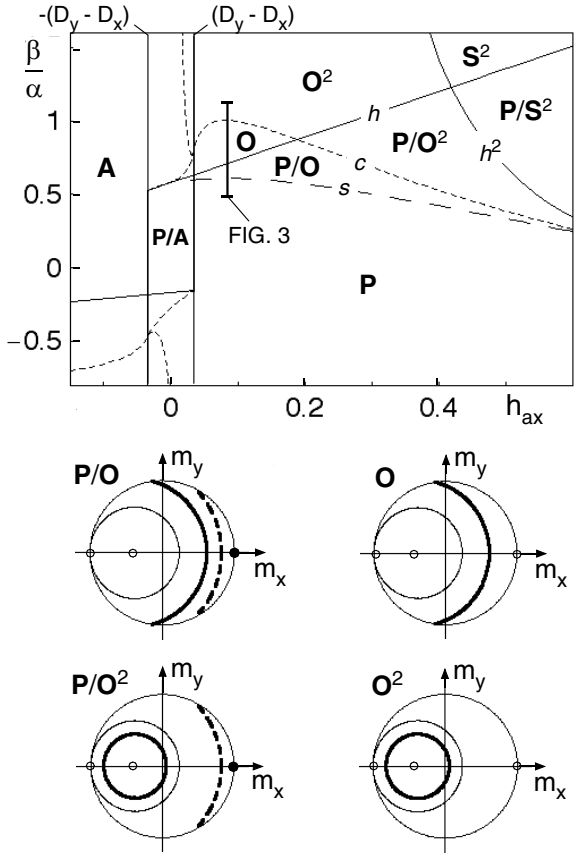

FIG. 2. Top Dynamical stability diagram for Eq. (1) when a field is applied along the easy axis (see text for description of symbols). System parameters: $D_x = -0.034$, $D_y = 0$, $D_z = 0.68$, $P = 0.3$, $d = 3$ nm, $\mu_0 M_s = 1.76$ T (these parameters refer to sample 2 of Ref. [7]; in that case, $\beta/\alpha = 1$ for a current of 5.6 mA). Vertical bar: current interval considered in Fig. 3. Bottom Schematic representation (see Fig. 1) of current-induced dynamical regimes. Solid circles: stable state at $m_x = 1$; open circles: unstable states; bold lines: stable limit cycle; bold dashed lines: unstable limit cycle.

will discuss the case $h_{ax} > D_y - D_x$ only. The bold symbols in Fig. 2 identify the regions of occurrence of the various dynamic regimes induced by the injection of the current. More precisely, **A** and **P** indicate the regions where the states $m_x = -1$ and $m_x = 1$ are stable, respectively; **O** where a stable limit cycle exists in the low-energy section L of the phase portrait shown in Fig. 1; $\mathbf{O}^2$ where two symmetric stable limit cycles are present in the sections H^2 of the phase portrait; $\mathbf{S}^2$ where two symmetric stable stationary states are present inside H^2. The slash notation (e.g., in $\mathbf{P}/\mathbf{O}$) indicates the coexistence of more than one stable state.

Under zero current, $m_x = 1$ is the only stable state. When a positive current is injected, the critical condition is reached where a pair of stable and unstable limit cycles appears inside L (semistable limit-cycle bifurcation [9]). Since limit cycles are zeros of the function $M(g_0, \mathbf{h}_a, \beta/\alpha)$, this bifurcation occurs when $M(g_0, \mathbf{h}_a, \beta/\alpha) = 0$, $\partial M(g_0, \mathbf{h}_a, \beta/\alpha)/\partial g_0 = 0$. Line s in Fig. 2 was obtained by solving this set of equations with respect to g_0 and β/α for different values of h_{ax}. The two limit cycles move apart from each other when the current is further increased. At some critical current, when the unstable limit cycle is reduced to the point $m_x = 1$, a Hopf bifurcation [9] occurs and the state $m_x = 1$ becomes unstable. By applying standard stability analysis to Eq. (1), one finds that this bifurcation occurs along the straight line: $\beta/\alpha = (1 + c_p)[h_{ax} + (D_z + D_y - 2D_x)/2]$ (line h in Fig. 2). The stability analysis also yields a simple expression for the angular frequency ω associated with the limit cycle disappearing at the bifurcation. In units of γM_s, this frequency is

$$\omega = \sqrt{[h_{ax} + (D_y - D_x)][h_{ax} + (D_z - D_x)]}, \qquad (5)$$

which strikingly coincides with the Kittel formula for ferromagnetic resonance [11]. Small-amplitude oscillations with this frequency are expected to appear when the system is close enough to the Hopf bifurcation. This is in fact what has been observed in experiments [7]. The validity of the Kittel formula is the natural consequence of the fact that the limit cycles of the current-driven dynamics reflect the free oscillations of the conservative dynamics.

The stable limit cycle formed at the semistable limit-cycle bifurcation moves toward and eventually reaches the boundary of L (homoclinic saddle-connection bifurcation [9]). In this case the bifurcation condition is $M(g_c, \mathbf{h}_a, \beta/\alpha) = 0$, where $g_c = D_x/2 + h_{ax}$ is the value of g_L at the boundary of L. Line c in Fig. 2 was determined by solving this equation for β/α as a function of the field. At the bifurcation point, the limit cycle spilts into two symmetric limit cycles which simultaneously appear in regions H^2. When the system is in the $\mathbf{P}/\mathbf{O}^2$ or $\mathbf{O}^2$ regime and the current is further increased, the stable limit cycles present in regions H^2 progressively shrink until they vanish at the energy maxima through a double Hopf bifurcation which transforms the energy maxima into stable out-of-plane stationary states. These states are indicated by $\mathbf{S}^2$ in Fig. 2 and the associated bifurcation line is labeled by h^2. No limit cycles are present anymore under such large fields and currents.

The outlined approach leads not only to the determination of the bifurcation lines where qualitative changes occur in the system response, but also to detailed predictions for the time-dependent magnetization vector $\mathbf{m}(t)$ associated with self-oscillations. This is obtained by analytically solving the equation $d\mathbf{m}/dt = -\mathbf{m} \times \mathbf{h}_{\text{eff}}$ and by using in the resulting solution $\mathbf{m}(t; g_0, \mathbf{h}_a)$ the values of g_0 obtained by solving the equation $M(g_0, \mathbf{h}_a, \beta/\alpha) = 0$ [12]. Figure 3 shows an example of the predicted magnetization response under varying positive current. For small currents the system is in the $m_x = 1$ state and the system response is time independent. The frequency f plotted in Fig. 3 for this

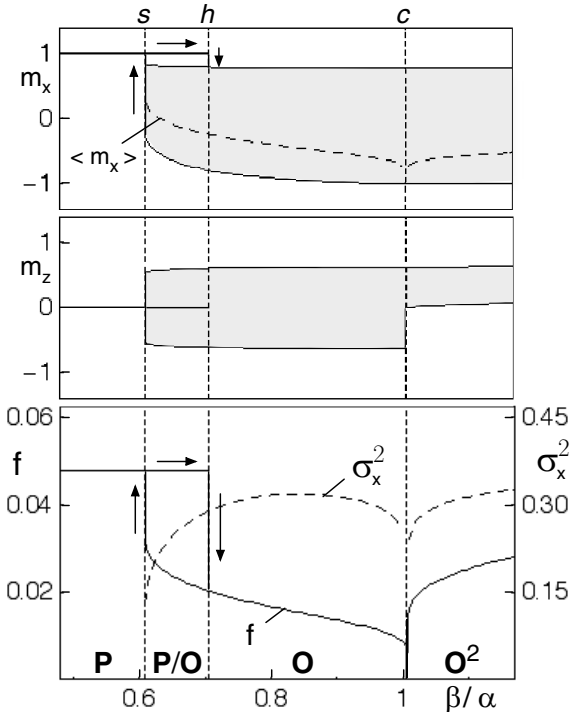

FIG. 3. Magnetization response for the system shown in Fig. 2 under varying current and $h_{ax} = 0.08$ (see text for description of symbols). Vertical dashed lines: bifurcation points. Arrows indicate hysteretic response. Top Gray regions: range of variation of m_x and m_z during self-oscillations; dashed line: time average $\langle m_x \rangle$. Bottom Solid line: self-oscillation frequency f in units of γM_s; dashed line: variance $\sigma_x^2 = \langle m_x^2 \rangle - \langle m_x \rangle^2$ for self-oscillations.

state is the frequency of the small-amplitude oscillations mentioned in relation to Eq. (5). At the Hopf bifurcation point where $m_x = 1$ becomes unstable the system jumps to the stable limit cycle present in L. This results in the sudden appearance of large-amplitude self-oscillations. Figure 3 shows that the self-oscillation frequency is a decreasing function of the current up to the saddle-connection bifurcation point. Here, as previously mentioned, the stable limit cycle splits into two symmetric out-of-plane limit cycles. A spontaneous symmetry breaking occurs in the magnetization response, with the appearance of out-of-plane self-oscillations (see plot of m_z in Fig. 3). From this point on, the self-oscillation frequency becomes an increasing function of the current. When the current is decreased starting from large values, the system reversibly reproduces previous self-oscillations until it enters the **P/O** regime, where stationary and self-oscillation stable states coexist. Here the response is hysteretic, with the self-oscillations persisting down to lower currents when the current is decreased. The **P/O** regime is where thermally induced transitions between coexisting states [3] and the related appearance of random-telegraph signals [5] are expected. These phenomena, not taken into account by the present zero-temperature approach, can be described by adding a random component to the effective field in Eq. (1).

The outlined approach is general and valid for all combinations of field and current, provided the free-layer magnetization can be assumed to be spatially uniform. We have used it to construct stability diagrams for a number of situations different from those shown in Fig. 2, for example, when the field and the current are both negative or the field is perpendicular to the free layer. These and other aspects will be discussed elsewhere.

This work was supported by MIUR-FIRB contract no. RBAU01B2T8, by CRT-ISI Lagrange, and by the US Department of Energy.

[1] J. C. Slonczewski, J. Magn. Magn. Mater. **159**, L1 (1996).
[2] L. Berger, Phys. Rev. B **54**, 9353 (1996).
[3] E. B. Myers, D. C. Ralph, J. A. Katine, R. N. Louie, and R. A. Buhrman, Science **285**, 867 (1999); J. A. Katine, F. J. Albert, R. A. Buhrman, E. B. Myers, and D. C. Ralph, Phys. Rev. Lett. **84**, 3149 (2000); E. B. Myers *et al.*, Phys. Rev. Lett. **89**, 196801 (2002).
[4] J. Grollier *et al.*, Appl. Phys. Lett. **78**, 3663 (2001); J. Grollier *et al.*, Phys. Rev. B **67**, 174402 (2003); B. Oezyilmaz *et al.*, Phys. Rev. Lett. **91**, 067203 (2003).
[5] S. Urazhdin, N. O. Birge, W. P. Pratt Jr., and J. Bass, Phys. Rev. Lett. **91**, 146803 (2003).
[6] W. Weber, S. Riesen, and H. C. Siegmann, Science **291**, 1015 (2001); H. Xi, K. Z. Gao, and Y. Shi, Appl. Phys. Lett. **84**, 4977 (2004); W. H. Rippard, M. R. Pufall, S. Kaka, S. E. Russek, and T. J. Silva, Phys. Rev. Lett. **92**, 027201 (2004).
[7] S. I. Kiselev *et al.*, Nature (London) **425**, 380 (2003).
[8] J. Z. Sun, Phys. Rev. B **62**, 570 (2000); S. Zhang, P. M. Levy, and A. Fert, Phys. Rev. Lett. **88**, 236601 (2002); Z. Li and S. Zhang, Phys. Rev. B **68**, 024404 (2003); M. D. Stiles and A. Zangwill, Phys. Rev. B **66**, 014407 (2002); Ya. B. Bazaliy, B. A. Jones, and Shou-Cheng Zhang, Phys. Rev. B **69**, 094421 (2004).
[9] L. Perko, *Differential Equations and Dynamical Systems* (Springer, Berlin, 1996); J. H. Hubbard and B. H. West, *Differential Equations: a Dynamical Systems Approach* (Springer, Berlin, 1995).
[10] In general, the phase portrait exhibits 6 energy extrema, of which 2 are saddles, for $|h_{ax}| < D_y - D_x$, 4 extrema (1 saddle) for $D_y - D_x < |h_{ax}| < D_z - D_x$, and 2 extrema (0 saddles) for $|h_{ax}| > D_z - D_x$. Only the intermediate case is addressed in this Letter.
[11] A. G. Gurevich and G. A. Melkov, *Magnetization Oscillations and Waves* (CRC Press, Boca Raton, 1996).
[12] Exact analytical solutions for the conservative dynamics were obtained through an extension of the method proposed by G. Bertotti, I. D. Mayergoyz, and C. Serpico, Physica B (Amsterdam) **343**, 325 (2004). The detailed calculations are quite involved and will be published elsewhere.